

ELECTROTONIC COUPLING OF SOMA AND AXON IN THE *APLYSIA* R2 NEURON

DOUGLAS JUNGE

*School of Dentistry, Department of Physiology and Brain Research Institute,
University of California, Los Angeles, California 90024, U.S.A.*

(Received September 18, 1984)

Abstract

The passive spread of inward (hyperpolarizing) current was studied in the giant neuron in the visceral ganglion of *A. californica*. Charging curves of soma potential vs. time during application of small inward current steps were only approximately fitted by single exponential functions. Charging curves were better fitted by the Rall theory, but equally good fits could be obtained over a sixfold variation of ρ , the axon/soma conductance ratio, by small adjustments of the membrane time constant. Curves of $\ln(\sqrt{t} dV/dt)$ vs. time could likewise be fitted by the Rall theory, with a similar uncertainty in ρ . In order to better determine the axon/soma coupling ratio, the input resistance, length constant and time constant were measured directly in several axons. A numerical model was then constructed in which the soma was represented by a single RC section and the axon by fifty additional sections. Somatic charging curves were well fitted by this model. The charging curves were best fitted when the length-specific internal resistance of the initial segment was less than that in the remainder of the axon. This finding could account in part for the larger length constant measured with one electrode in the soma and one in the axon than with both in the axon.

1. Introduction

In early studies of the electrical properties of mollusc neurons, each cell was considered to be an isopotential structure and the axon was largely ignored (Tauc, 1955; Arvanitaki and Chalazonitis, 1961; Murray, 1966). Then, in 1962, Tauc found that action potentials in the R2 neuron originated in the axon about 1 mm from the soma, and that there was a region extending 500 μm or more from the soma which at times could not conduct antidromic action potentials. Coggeshall (1967) has published a picture of a typical *Aplysia* neuron, based on electronmicrographs, in which the initial portion of the axon (or trophospongium) is broken up into small processes which are completely interdigitated with glial cells. This may in fact be the inexcitable region found by Tauc. As shown by Gillette and Pomeranz (1973) with dye injection, the R2 axon branches less than 1 mm from the soma, and sends its major telodendron into the right connective and a smaller branch into the branchial nerve. However, the cross-sectional area of this branch is less than 1% of that of the main axon, so it would not be expected to conduct more than 1% of currents reaching the branch point.

Using one recording electrode in the soma and one in the axon, various authors have reported that the length constant of the R2 axon is 4.3 mm (Tauc, 1962), 10 mm (Junge and Miller, 1974) and about 5 mm (Miller, 1875; Horn, 1977). While such

measurements depend on the amount of stretch applied to the visceropleural connective which contains the axon, they are all larger than was found in the present study (2.1 mm) with both recording electrodes in the axon. This disparity may also reflect the different properties of the trophospongium and the rest of the axon.

The first description of the effects of axon cable properties on the electrical characteristics of a whole neuron was given by Rall (1960). This theory has been extended and applied to a variety of neurons, including some in molluscs (Gorman and Mirolli, 1972; Graubard, 1973, 1975). The principal drawbacks to applying this theory to the R2 cell are (1) it is difficult to estimate the time constant accurately when the axon/soma conductance ratio, ρ , is less than 2 (Rall, 1960), and (2) the theory assumes that the time constant is the same in the cell body and axon, which is not supported by measurements in R2 neurons.

It has been of concern to electrophysiologists to know, when current is injected into a nerve cell body, how much of it flows into the axon. The results of the present study indicate that this cannot be uniquely determined for the R2 cell by Rall analysis, and that a better approximation is given by a numerical approach based on direct measurement of axonal parameters.

2. Methods

The animals used in this study measured approximately 15–20 cm in length. The visceral ganglion, with more than 4 cm of the right connective attached, was removed and pinned in an 8-cm-long polystyrene chamber (volume = 5 cc). The preparation was treated with a 1% solution of pronase in normal saline for 15–20 min. at room temperature, as an aid to impalement. Following washing with saline, the cell soma was impaled with recording and stimulating electrodes of resistance 2–4 M Ω , filled with 3M KCl. To impale the axon, regular pulses were first applied to the soma to produce action potentials. The axon was then located by searching across the connective with another recording electrode, and impaled when large extracellular signals were seen. Two microelectrodes were placed in the axon about 3–5 mm apart, both of them more than 1 cm from the ganglion. To measure input resistance and time-constant, a known current was injected via the proximal electrode with a stimulus-subtracting circuit (W-P Instruments Model M701), and the resulting potential change recorded in the same electrode. The potential change in the other axonal electrode, a known distance from the first, was used to estimate the length constant. Somatic potential traces were differentiated using a single operational amplifier circuit with a time constant of 8 msec. Data were collected both by photographing traces on the oscilloscope and by A/D conversion (Northwest Instrument Systems Model 85 aScope) and storage in binary form on diskettes. Digitized records could then be compared directly with theoretical curves on the video monitor. Several of the figures in this report were produced by “dumping” the monitor screen to an Epson Model FX-80 printer.

The normal saline used had the composition NaCl 450 mM, KCl 10 mM, CaCl₂ 11 mM, MgCl₂ 49 mM, Tris HCl (pH 7.7) 10 mM. Experiments were carried out throughout the year at room temperature (20–23°C). R2 soma diameters were

estimated with a calibrated eyepiece. This was only a rough measurement, as the somas were often ellipsoidal in shape.

3. Results

Electrical properties of cells with attached axons

Figure 1 indicates the type of data analyzed in this study. Part A shows the response of an R2 cell to a 0.9-s inward step of current. The record of dV/dt is close to an inverted version of the potential trace, but differs because the potential does not follow a single exponential function of time, as will be discussed below. The potential changes resulting from applied current steps of various amplitudes are shown in Part B. (Hyperpolarizations were used to avoid activation of voltage-sensitive conductances.) In the range $0 < V < 24$ mV, the current-voltage relation was approximately linear. Hence, throughout this study, potential changes of less than 22 mV were used, to avoid the increase in conductance, or inward rectification, known to occur at more negative potentials (Eaton and Brodwick, 1976).

To determine whether the charging curves of somatic potential could be represented by a single exponential function, the data was plotted as shown in Figure 2. The inset shows digitized potential and current records. If the potential follows a single exponential, then the function plotted as ordinate should be linear with time and pass through the origin. That this was not the case suggested that the attached axon was modifying the electrical properties of the cell body.

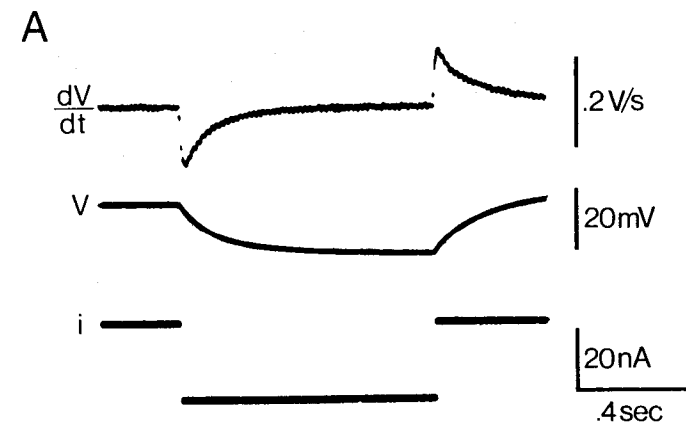
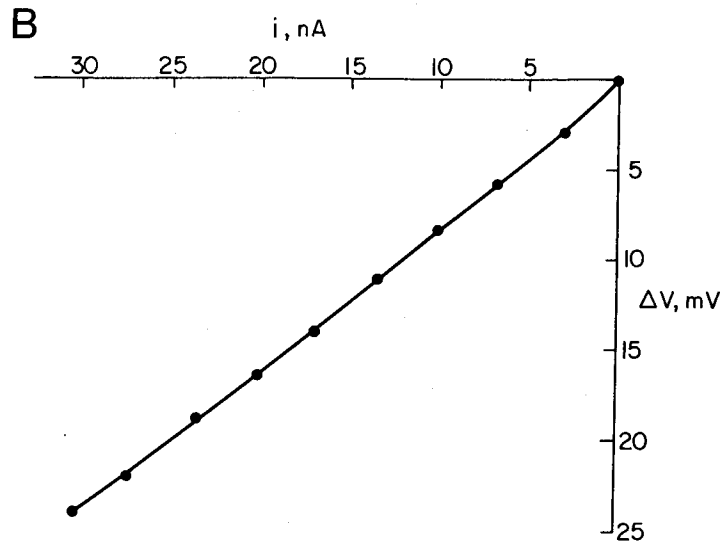


Fig. 1. Potential response of R2 cell with attached axon to step of inward current applied to soma. Part A: dV/dt shows electronically obtained time derivative of potential trace, V , i = applied current.



Part B: Current-voltage relation. ΔV = final value of potential V_f above, vs. applied current.

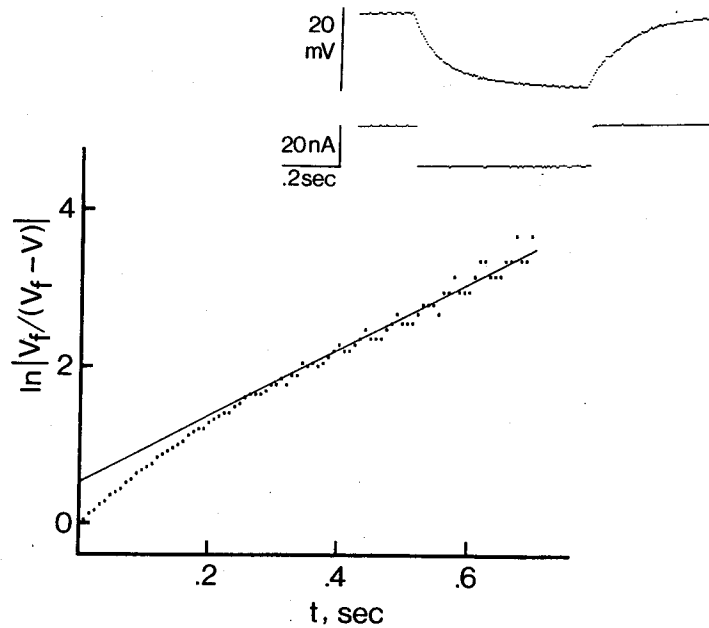


Fig. 2. Non-exponential time-course of somatic charging curve. Inset shows digitized potential and current traces. Dots in graph below are same potential data plotted as shown on ordinate.

Table I shows a summary of some electrical constants obtained for ten cells with attached axons. The time constant was estimated as if the potential curves followed single exponential functions, i.e., the time to reach 0.632 of the final value; however, this was just an approximation as mentioned above. Some variation of input resistance ($= V_f/I$) was seen, larger resistances generally being associated with smaller soma diameters. (It was interesting that, in earlier data obtained from 11 cells whose

Table I. Electrical properties of cells with attached axons. Values below: mean \pm S.D. Diam. = largest diameter measured with ocular scale on microscope. τ_s = time for somatic potential to reach $0.632 \times$ final value. R_{in} defined in text.

Cell	Diam.	τ_s	R_{in}
10-23	—	0.11 s	1.18 M Ω
10-30	—	0.17	1.43
12-15	620 μ m	0.16	0.847
1-3	400	0.14	1.65
1-5	500	0.13	0.708
1-9	620	0.06	0.267
1-13	430	0.09	0.816
1-19	600	0.13	0.849
1-25	560	0.155	1.09
1-30	530	0.165	0.898
	532 ± 84	0.131 ± 0.036	0.97 ± 0.39

axons had been cut off within 3 mm of the ganglion, the mean input resistance was only 0.62 M Ω . This suggested that the cut ends of the axons did not seal completely. It was not possible with this preparation to completely remove the axon and study the properties of an isolated soma.)

Rall theory

One approach which could account for the axonal loading of somatic potential responses was that of Rall (1960). The procedure usually employed here is to examine the function

$$\ln(\sqrt{t} \, dV/dt) \text{ vs. } t$$

at late times. The inverse negative slope of this line is the time constant, τ . Then the function

$$\ln \left[\sqrt{t} \, V_f \frac{\rho+1}{\tau} e^{\rho^2-1)/\tau} \operatorname{erfc}(\rho\sqrt{t}/\tau) \right]$$

(where V_f = final value of potential) is fitted to the entire curve of $\ln(\sqrt{t} \, dV/dt)$ by suitable choice of ρ . This is shown for an R2 cell in Figure 3. In the upper graph, a line was fitted to the data at $t > 0.2$ s which gave a τ of 0.18 s. When ρ was set to 0.2, this gave a not unreasonable fit to the function $\ln(\sqrt{t} \, dV/dt)$. However, when the slope at late times was adjusted to make $\tau = 0.225$ s, the data was only fitted if ρ was chosen equal to 1.3.

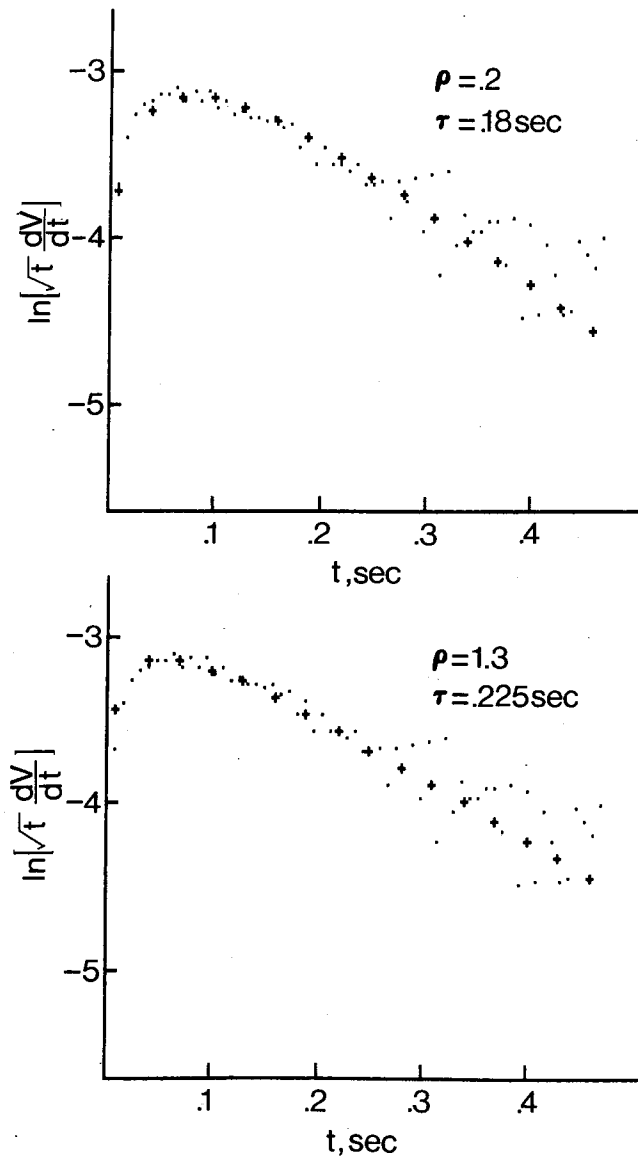


Fig. 3. Fits of Rall equation to the function $\ln(\sqrt{t} dV/dt)$ vs. t . Dots show observed data, pluses solution of Rall equation given in text. Top graph: Axon/soma conductance ratio, ρ , assumed equal to 0.2; time-constant, τ , equal to 0.18 s. Bottom: Assuming slightly larger τ requires that $\rho = 1.3$ for good fit to data. $V_f = -0.019 \text{ V}$.

The Rall equation for the somatic potential change in response to a step of current is

$$(1) \quad V(t) = \frac{V_f}{\rho - 1} [\rho \operatorname{erf}(\sqrt{t/\tau}) - 1 + e^{(\rho^2 - 1)t/\tau} \operatorname{erfc}(\rho\sqrt{t/\tau})]$$

This is fitted in Figure 4 to the observed potential curve with the two different values of τ and ρ used in Figure 3. Both sets of parameters gave reasonable fits to the

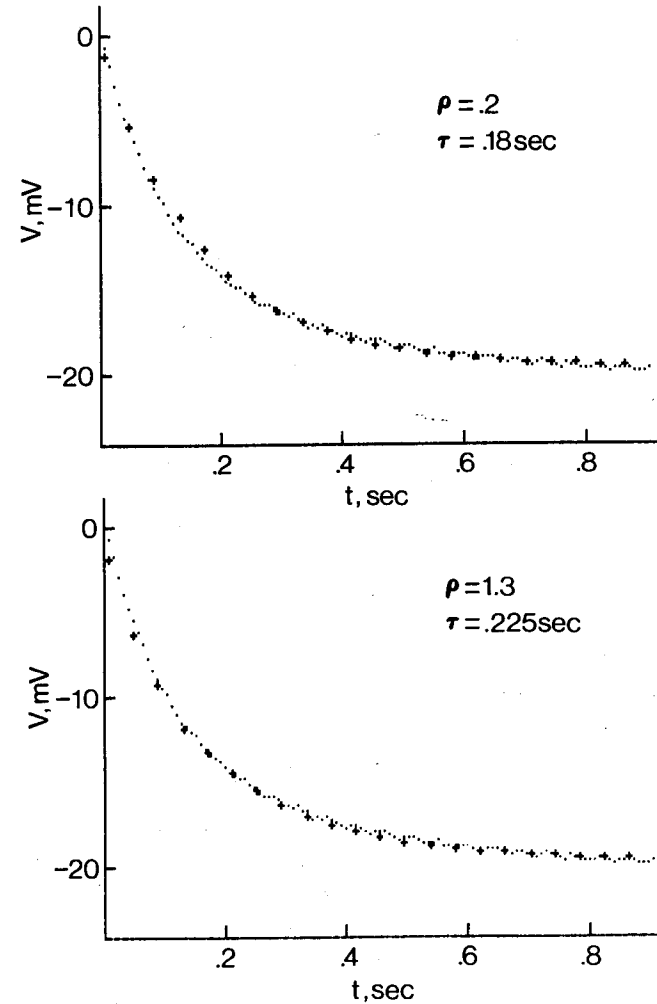


Fig. 4. Fits of Eqn. 1 for potential charging curves (pluses) to observed data (dots). Same values of τ , ρ and V_f as in Fig. 3.

potential curves. Thus, based on these fits of the Rall theory to the observed data, the axon end-conductance might be anything from 0.2 to 1.3 times the somatic conductance.

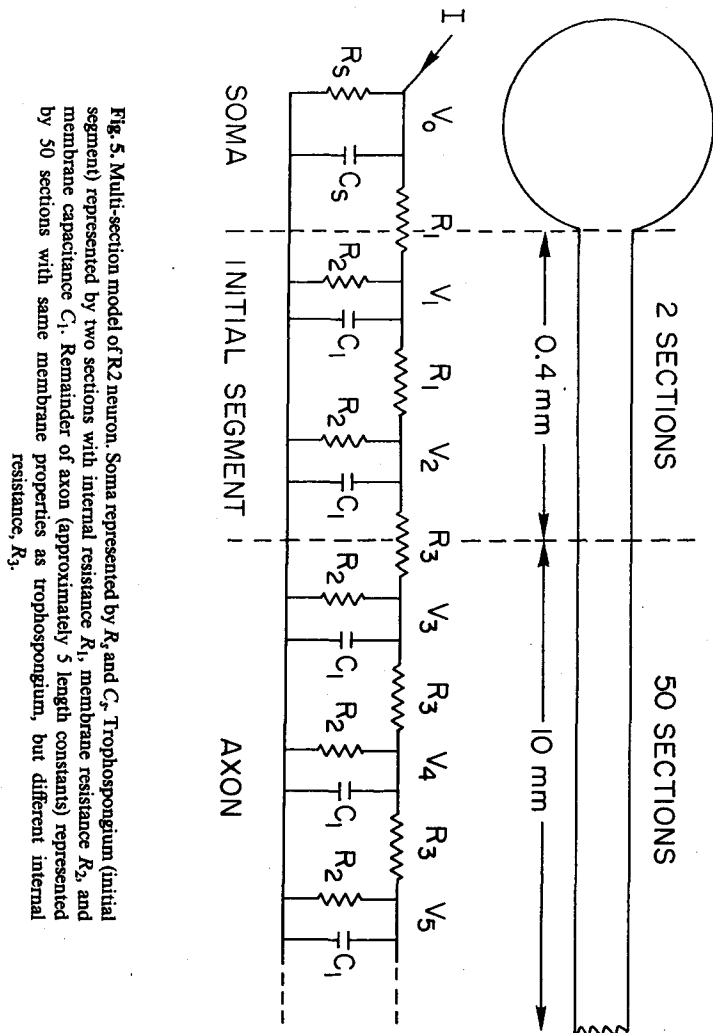


Fig. 5. Multi-section model of R2 neuron. Soma represented by R_s and C_s . Trophosphonium (initial segment) represented by two sections with internal resistance R_1 , membrane resistance R_2 , and membrane capacitance C_1 . Remainder of axon (approximately 5 length constants) represented by 50 sections with same membrane properties as trophosphonium, but different internal resistance, R_3 .

Multi-section model

In order to obtain a more quantitative measure of the fraction of conductance contributed by the axon, a numerical model was constructed, as shown in Figure 5. The cell body was represented by a single RC section with resistance R_s and capacitance C_s . The axon was modeled by 52 connected RC sections, each representing 0.2 mm of length. The internal resistivity, R_1 , of the first two sections could be varied independently. The equations describing the behavior of this model are of the form

$$(2) \quad \dot{V}_0 = (I - V_0/R_s - V_0/R_1 + V_1/R_1)/C_s$$

$$(3) \quad \dot{V}_1 = (V_0/R_1 - 2V_1/R_1 - V_1/R_2 + V_2/R_1)/C_1$$

$$\vdots$$

$$(4) \quad V_0(t + \Delta t) = V_0(t) + \dot{V}_0 \Delta t$$

$$(5) \quad V_1(t + \Delta t) = V_1(t) + \dot{V}_1 \Delta t$$

$$\vdots$$

Equations 4 and 5 represent the Euler method of solution of the simultaneous differential equations. The solution is stable with this method if $\Delta t < 0.001$ s.

Electrical properties of axons

To obtain axonal parameters for use in this model, two-electrode axon experiments were carried out as described in the Methods. Figure 6 shows the voltage changes at

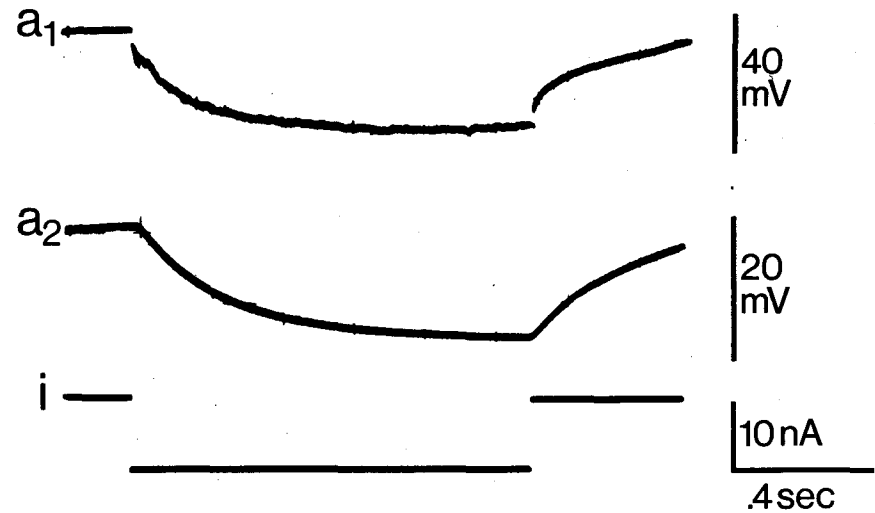


Fig. 6. Response of R2 axon at two different points to current step applied at one of these points. a_1 : Potential recorded at stimulating site, 1 cm from soma, with stimulus-subtracting circuit. a_2 : Potential recorded 3 mm distal to first site. i : Applied current.

the site of application of a current step (a_1) and at a second electrode 3 mm further from the soma (a_2). The time constant (equal to the time to rise to $0.843 \times$ final value) and input resistance were obtained from the first record and the length constant by comparing the final values of both. Table II compares these parameters in several

Table II. Electrical properties of axons. Values below: mean \pm S.D. τ = time to reach $0.843 \times$ final value of potential. R_{in} and λ defined in text.

Axon	τ	R_{in}	λ
9-24	0.33s	0.60 M Ω	—
10-7	0.50	0.40	—
10-23	0.33	2.42	—
10-30	0.29	1.74	—
5-22	0.33	3.0	0.22 cm
6-2	0.25	3.2	0.11
6-8	0.20	2.36	0.28
1-9	0.22	0.89	0.22
	0.31 ± 0.094	1.82 ± 1.09	0.208 ± 0.071

different axons. (Note that the time constant is much larger than that found for the whole neurons in Table I. Assuming the somatic time constant is close to that found for the soma with axon attached, this difference contradicts the assumption in the Rall theory that the axonal and somatic time constants are identical.)

The values of the model parameters were then calculated as follows:

The values of λ and R_{in} were given by

$$(6) \quad \lambda = \sqrt{r_m/r_i}$$

$$(7) \quad R_{in} = 1/2 \sqrt{r_m \cdot r_i}$$

where

r_m = length-specific membrane resistance, $\Omega \cdot \text{cm}$,

r_i = length-specific internal resistance, Ω/cm .

The time-constant, τ , was

$$(8) \quad \tau = r_m c_m$$

where c_m = length-specific capacitance, F/cm.

These were solved to find

$$r_m = 7.57 \times 10^5 \Omega \cdot \text{cm}$$

$$r_i = 1.749 \times 10^7 \Omega/\text{cm}$$

$$c_m = 4.095 \times 10^{-7} \text{ F/cm}$$

The model values R_2 , R_3 and C_1 were found by multiplying or dividing by 0.02 cm/section . R_5 and C_5 were taken as $1 \text{ M}\Omega$ and $1.5 \times 10^{-7} \text{ F}$ for the cell modeled.

Model predictions and currents in the model

The somatic charging curve predicted by this model when $R_1 = R_3 = 3.5 \times 10^5 \Omega$ is shown in Figure 7, in the top graph. The charging curve observed in the R2 neuron

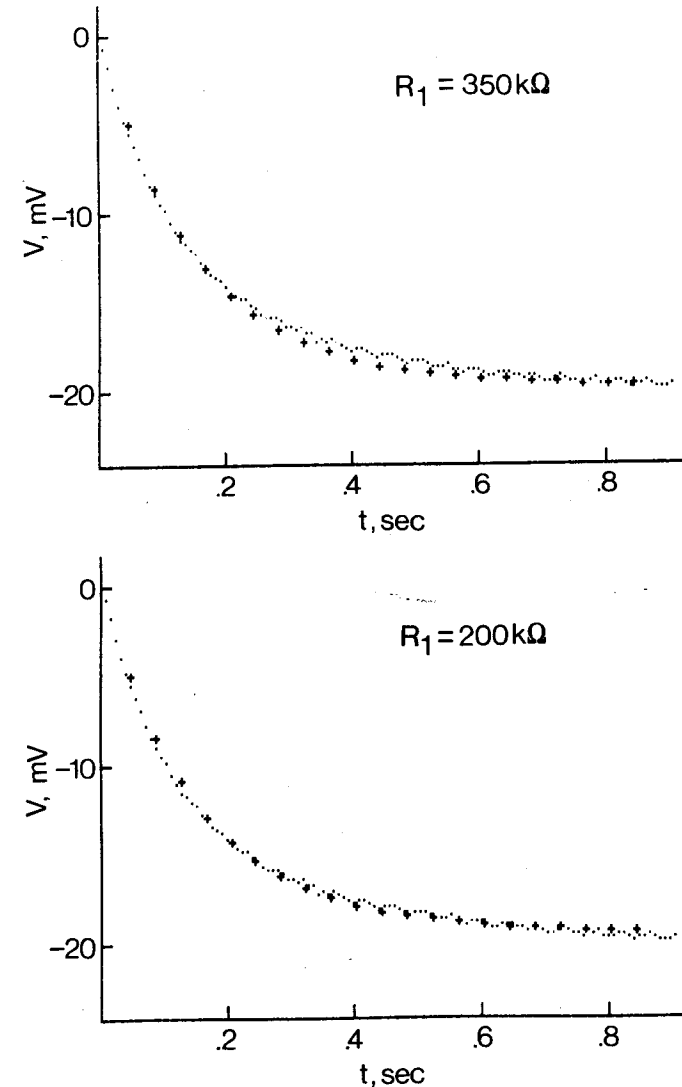


Fig. 7. Fits of multi-section model (pluses) to observed somatic charging curves (dots). Top graph: fit obtained with measured axon parameters. Bottom graph: fit obtained when internal resistance of first two axon segments assumed smaller, as shown. $I = 10^{-8} \text{ A}$; $R_5 = 10^6 \Omega$; $C_5 = 1.5 \times 10^{-7} \text{ F}$; $R_2 = 3.79 \times 10^7 \Omega$; $R_3 = 3.5 \times 10^5 \Omega$; $C_1 = 8.19 \times 10^{-9} \text{ F}$.

was about 4% more positive than the model curve at 0.4 s, but it was reasonably well approximated by the model. When the internal resistance of the initial two segments, R_1 , was changed to $2.0 \times 10^5 \Omega$, the improved fit shown in the bottom graph was produced. (A smaller length-specific internal resistance in the trophospongium might be due to a greater net cross-sectional area of the axon processes in that region than of the distal axon.) Thus, the multi-section model with measured axon parameters gave a good representation of the charging curve in response to a step of current applied to the soma.

In order to examine the distribution of currents throughout the neuron, the axon current i_a , equal to $(V_0 - V_1)/R_1$ in the model, was plotted separately from the soma current, i_s , and total current as shown in Figure 8. The initial peak in the soma current was due to charging of the somatic capacitance. After the soma and end-axon currents had become constant, the somatic potential continued to increase as more and more of the axon membrane was polarized, with the measured parameters, and assuming

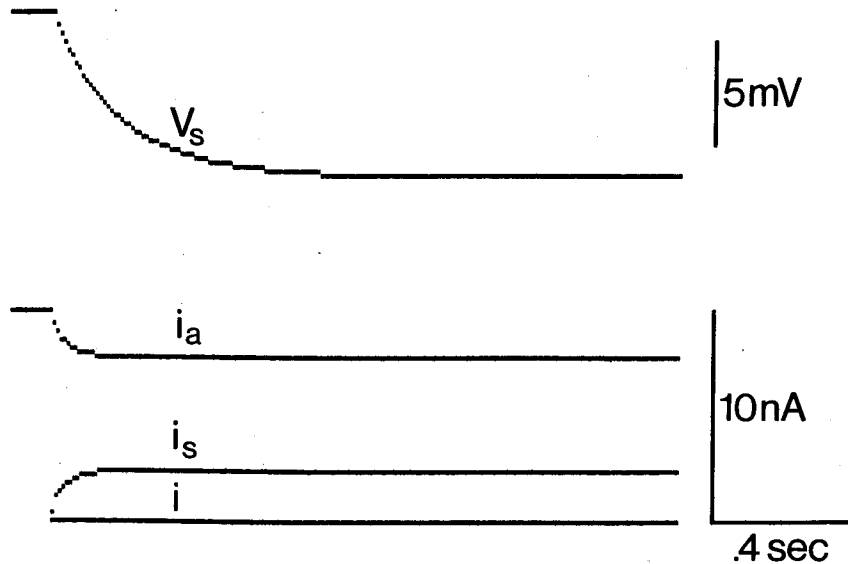


Fig. 8. Distribution of applied current between soma and axon in the model. V_s : somatic charging curve in response to current step, i_a : axonal current, equal to $(V_0 - V_1)/R_1$. i_s : somatic current, equal to $i - i_a$.

$R_1 = 2.0 \times 10^5 \Omega$, the final ratio i_a/i_s was 0.282. For the "average cell" in the study, the whole neuron conductance from Table I was $1.03 \mu S$, the axon end-conductance was $0.275 \mu S$, and the somatic conductance was $0.755 \mu S$. Thus the average ρ was 0.364. This may be considered a more reliable measure of the axon/soma conductance ratio than was obtained with Rall analysis, for the reasons mentioned above.

The effect of decreasing the length-specific internal resistance on the soma-axon coupling is shown in Figure 9. V_s shows the potential change at the soma, and V_a that in the axon at about one length-constant (10 sections) from the soma. Decreasing R_1 as shown had the effect of decreasing the somatic potential change and increasing the axonal response. Thus, decreasing the internal resistance of the trophospongium increased the length constant. While the value of this internal resistance is not known for real R2 neurons, assuming it to be smaller than in the distal axon (1) gives improved fits to somatic charging curves, and (2) can in part explain the larger length-constant found with soma-to-axon measurements.

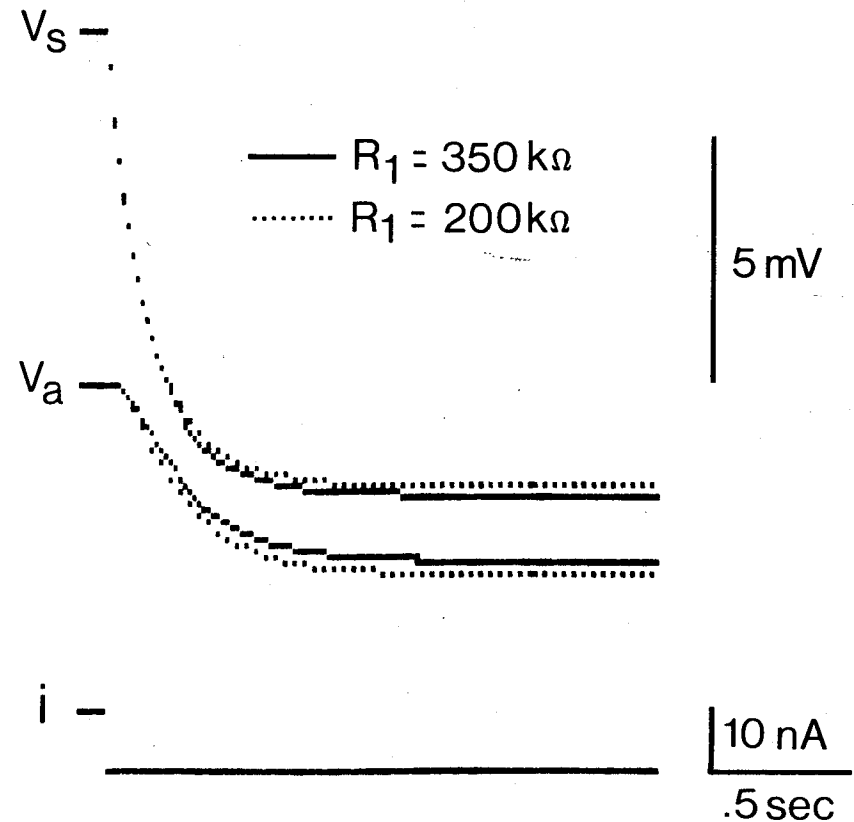


Fig. 9. Effect of internal resistance in trophospongium region on length constant measured from soma to axon. V_s : somatic potential. V_a : axon potential at 10 sections (approximately one length constant) from soma. See text for details.

4. Discussion

The principal finding in this report is that in the non-activated R2 cell an applied current divides into a somatic current and an axonal current which is about 36% of the somatic current. (This means the axonal current is only 27% of the total current.) It provides, in a broad sense, a justification for treating the neuron almost as a single RC section. (But note that with the Rall fit in Figure 4, the axonal current was 130% of the somatic current, and 56% of the total current!)

It is possible to obtain estimates of area-specific parameters from the measurements obtained in this study: For the "average soma", the area of a sphere with this diameter is $8.89 \times 10^{-3} \text{ cm}^2$. If the specific capacitance, C_m , is $1 \mu\text{F}/\text{cm}^2$, this indicates a total somatic capacitance, C_s , of $8.89 \times 10^{-9} \text{ F}$. The average resistance of the soma, R_s , should be equal to $(1 + \rho)R_{in}$, or $1.32 \text{ M}\Omega$. Dividing the measured value of τ_s by this gives a value of C_s of $9.92 \times 10^{-8} \text{ F}$. The apparent excess capacitance over that found above is considered to be due to infolding of the somatic membrane, in this case by a factor of $11.2x$. Assuming the increased somatic area of 0.0996 cm^2 , this yields an R_m for the soma of $1.31 \times 10^5 \Omega \cdot \text{cm}^2$. This agrees with previous estimates of R_m in mollusc neurons (Carpenter, 1970; Marmor, 1971).

To calculate the area-specific parameters in the axon, it is necessary to use the formulation of Mirolli and Talbott (1972) to include the effects of infolding. The length constant is given by

$$(9) \quad \lambda = \sqrt{\frac{A}{P}} \sqrt{\frac{R_m}{R_i}}$$

and the input resistance is

$$(10) \quad R_{in} = 1/2 \frac{\sqrt{R_m \cdot R_i}}{\sqrt{A \cdot P}}$$

Where

A = area of axon cross-section

P = perimeter of cross-section

Values of A and P were obtained by planimetric measurement of two cross sections of the R2 axon published by Pinsker *et al.* (1976). They were:

Section	$A, \text{ cm}^2$	$P, \text{ cm}$
I	1.53×10^{-5}	0.184
II	1.49×10^{-5}	0.206

The fact that the A/P ratio is similar in both sections suggests that a unidimensional model with constant λ is valid. Using the average A ($1.51 \times 10^{-5} \text{ cm}^2$) and P (0.195 cm), equations 9 and 10 can be solved to find $R_m = 1.48 \times 10^5 \Omega \cdot \text{cm}^2$ and $R_i = 264 \Omega \cdot \text{cm}$. The value of R_i is much larger than the $40 \Omega \cdot \text{cm}$ found by Foster *et al.* (1976) by impedance measurements in *Aplysia* cell bodies, but is closer to the values of up to $115 \Omega \cdot \text{cm}$ found by Hodgkin (1947) for crab axons. With the measured axon

time constant, 0.31 s, the area-specific capacitance, C_m , should be $2.09 \mu\text{F}/\text{cm}^2$. The variation of this from the usual value of $1 \mu\text{F}/\text{cm}^2$ may reflect some inaccuracy of the above morphometric measurements. A greater variation of A and P along the axon than was indicated by the two sections measured also cannot be ruled out at present.

To account for the larger value of λ when measured from soma to axon, equation 9 shows that there are four parameters which might be different in the proximal and distal axon. The possibility of an increased A in the proximal axon has been mentioned in the Results. It seems less likely that P would be smaller in the trophosphonium, where the axon breaks up into several processes. However, these processes might not be infolded as much as the distal axon. Finally, R_m and R_i may differ in the trophosphonium and main axon. In the model, it happens that decreasing R_i in the initial two segments has a much greater effect than increasing R_2 (the other way to increase λ), since not much current flows across the membrane in those sections. To show a strong effect of changing R_2 , several more sections would have to be included in the trophosphonium.

In conclusion, the type of cable model presented has an advantage over trying to infer axon/soma coupling ratios from charging curves and their time derivatives, in that the axon parameters are measured directly. The next step in developing the model will be to determine the axon-soma coupling under conditions when one or both regions are excited.

Acknowledgements

This work was supported by NIH Grant RR 05304. I thank J. Chad for reading the manuscript.

References

- Arvanitaki, A. and Chalazonitis, N. (1961). Slow waves and associated spiking in nerve cells of *Aplysia*. *Bull. Inst. Oceanogr. Monaco* **58**, 1-15.
- Carpenter, D. O. (1970). Membrane potential produced directly by the Na^+ pump in *Aplysia* neurons. *Comp. Biochem. Physiol.* **35**, 371-385.
- Coggeshall, R. E. (1967). A light and electron microscope study of the abdominal ganglion of *Aplysia californica*. *J. Neurophysiol.* **30**, 1263-1287.
- Eaton, D. C. and Brodwick, M. S. (1976). Inward rectification in *Aplysia* giant neurons. *Biophysic. J.* **16**, 24a.
- Foster, K. R., Bidinger, J. M. and Carpenter, D. O. (1976). The electrical resistivity of cytoplasm. *Biophysic. J.* **16**, 991-1001.
- Gillette, R. and Pomeranz, B. (1973). A study of neuron morphology in *Aplysia californica* using procion yellow dye. *Comp. Biochem. Physiol.* **44A**, 1257-1259.
- Gorman, A. L. F. and Mirolli, M. (1972). The passive electrical properties of the membrane of a molluscan neurone. *J. Physiol.* **227**, 35-49.
- Graubard, K. (1973). *Morphological and Electrotonic Properties of Identified Neurons of the Mollusc, Aplysia Californica*. Ph.D. Dissertation. University of Washington, Seattle.
- Graubard, K. (1975). Voltage attenuation within *Aplysia* neurons: the effect of branching pattern. *Brain Res.* **88**, 325-332.

- Hodgkin, A. L. (1947). The membrane resistance of a non-medullated nerve fibre. *J. Physiol.* **106**, 305-318.
- Horn, R. J. (1977). *Voltage Dependent Calcium Permeability in the Soma and Axon of Aplysia Giant Neuron: The Action of Tetraethylammonium*. Ph.D. Dissertation, University of California, Los Angeles.
- Junge, D. and Miller, J. (1974). Different spike mechanism in axon and soma of molluscan neurone. *Nature* **252**, 155-156.
- Marmor, M. (1971). The effects of temperature and ions on the current-voltage relation and electrical characteristics of a molluscan neurone. *J. Physiol.* **218**, 573-598.
- Miller, J. J. (1976). *Aplysia Giant Neuron: An Electrophysiological Comparison of the Soma and the Axon*. Ph.D. Dissertation, University of California, Santa Cruz.
- Mirolli, M. and Talbott, S. R. (1972). The geometrical factors determining the electrotonic properties of a molluscan neurone. *J. Physiol.* **227**, 19-34.
- Murray, R. W. (1966). The effect of temperature on the membrane properties of neurons in the visceral ganglion of *Aplysia*. *Comp. Biochem. Physiol.* **18**, 291-303.
- Pinsker, H., Feinstein, R., Sawada, M. and Coggeshall, R. (1976). Anatomical basis for an apparent paradox concerning conduction velocities of two identified axons in *Aplysia*. *J. Neurobiol.* **7**, 241-253.
- Rall, W. (1960). Membrane potential transients and membrane time constant of motoneurons. *Exp. Neurol.* **2**, 503-532.
- Tauc, L. (1955). Etude de l'activité élémentaire des cellules du ganglion abdominal de l'*Aplysie*. *J. Physiol. Par.* **47**, 769-792.
- Tauc, L. (1962). Site of origin and propagation of spike in the giant neuron of *Aplysia*. *J. Gen. Physiol.* **45**, 1077-1097.